The Astrophysical Journal, 727:15 (7pp), 2011 January 20 doi:10.1088/0004-637X/727/1/15

THE EXTREME HOSTS OF EXTREME SUPERNOVAE

James D. Neill[1], Mark Sullivan[2], Avishay Gal-Yam[3], Robert Quimby[1], Eran Ofek[1], Ted K. Wyder[1], D. Andrew Howell[4], Peter Nugent[5], Mark Seibert[6], D. Christopher Martin[1], Roderik Overzier[7], Tom A. Barlow[1], Karl Foster[1], Peter G. Friedman[1], Patrick Morrissey[1], Susan G. Neff[8], David Schiminovich[9], Luciana Bianchi[10], José Donas[11], Timothy M. Heckman[12], Young-Wook Lee[13], Barry F. Madore[6], Bruno Milliard[11], R. Michael Rich[14], and Alex S. Szalay[12]

[1] California Institute of Technology, 1200 E. California Blvd., Pasadena, CA 91125, USA
[2] University of Oxford, Denys Wilkinson Building, Keble Road, Oxford, OX1 3RH, UK
[3] Department of Particle Physics and Astrophysics, Faculty of Physics, Weizmann Institute of Science, 76100 Rehovot, Israel
[4] Las Cumbres Observatory Global Telescope Network, 6740 Cortona Dr., Suite 102, Goleta, CA 93117, USA
[5] Lawrence Berkeley National Laboratory, MS 50F-1650, 1 Cyclotron Road, Berkeley, CA 94720-8139, USA
[6] The Observatories of the Carnegie Institute of Washington, 813 Santa Barbara Street, Pasadena, CA 91101, USA
[7] Max-Planck-Institut für Astrophysik, Karl-Schwarzschild-Str. 1, D-85748 Garching, Germany
[8] Laboratory for Astronomy and Solar Physics, NASA Goddard Space Flight Center, Greenbelt, MD 20771, USA
[9] Department of Astronomy, Columbia University, New York, NY 10027, USA
[10] Center for Astrophysical Sciences, The Johns Hopkins University, 3400 North Charles Street, Baltimore, MD 21218, USA
[11] Laboratoire d'Astrophysique de Marseille, BP 8, Traverse du Siphon, 13376 Marseille Cedex 12, France
[12] Department of Physics and Astronomy, The Johns Hopkins University, Homewood Campus, Baltimore, MD 21218, USA
[13] Center for Space Astrophysics, Yonsei University, Seoul 120-749, Republic of Korea
[14] Department of Physics and Astronomy, University of California, Los Angeles, CA 90095, USA
Received 2010 September 7; accepted 2010 November 12; published 2010 December 23

ABSTRACT

We use *GALEX* ultraviolet (UV) and optical integrated photometry of the hosts of 17 luminous supernovae (LSNe, having peak $M_V < -21$) and compare them to a sample of 26,000 galaxies from a cross-match between the SDSS DR4 spectral catalog and *GALEX* interim release 1.1. We place the LSN hosts on the galaxy NUV $- r$ versus M_r color–magnitude diagram (CMD) with the larger sample to illustrate how extreme they are. The LSN hosts appear to favor low-density regions of the galaxy CMD falling on the blue edge of the blue cloud toward the low-luminosity end. From the UV-optical photometry, we estimate the star formation history of the LSN hosts. The hosts have moderately low star formation rates (SFRs) and low stellar masses (M_*) resulting in high specific star formation rates (sSFR). Compared with the larger sample, the LSN hosts occupy low-density regions of a diagram plotting sSFR versus M_* in the area having higher sSFR and lower M_*. This preference for low M_*, high sSFR hosts implies that the LSNe are produced by an effect having to do with their local environment. The correlation of mass with metallicity suggests that perhaps wind-driven mass loss is the factor that prevents LSNe from arising in higher-mass, higher-metallicity hosts. The massive progenitors of the LSNe ($>100\,M_\odot$), by appearing in low-SFR hosts, are potential tests for theories of the initial mass function that limit the maximum mass of a star based on the SFR.

Key words: galaxies: dwarf – stars: luminosity function, mass function – stars: massive – supernovae: general
Online-only material: color figures

1. INTRODUCTION

Two extremely luminous core-collapse (CC) supernovae (SNe) were recently discovered with faint or non-detected hosts, one at low redshift (SN2005ap, $M_{\rm Bol,Peak} = -22.7$ at $z = 0.283$; Quimby et al. 2007) and one with the *Hubble Space Telescope* at a higher redshift (SCP 06F6, $M_{\rm Bol,Peak} = -22.1$ at $z = 1.189$; Barbary et al. 2009; Quimby et al. 2009). Recent wide-area surveys (e.g., Quimby 2006; Rau et al. 2009; Law et al. 2009; Drake et al. 2009) have discovered similar objects revealing a new class of extremely luminous CC SNe (Quimby et al. 2007, 2010; Ofek et al. 2007; Smith et al. 2008; Yuan et al. 2008; Miller et al. 2009; Gezari et al. 2009; Gal-Yam et al. 2009; Drake et al. 2010; Pastorello et al. 2010) that were missed in earlier host-targeted surveys due to their preference for low-mass hosts (Young et al. 2010; Quimby et al. 2009; Gal-Yam et al. 2009). It is not uncommon that other types of extremely luminous SNe are found in low-luminosity hosts (see, e.g., Kozłowski et al. 2010), for example many extreme SNe IIn (see Section 2) seem to prefer dwarf hosts (Richardson et al. 2002; Smith et al. 2008; Miller et al. 2009), but not always (Smith et al. 2007).

The preference these extremely luminous SNe (LSNe) have for low-mass and presumably low-metallicity hosts implies a factor in their production specific to the host galaxy. It is thus important to begin to quantify the local host environments of the LSNe. The link between galaxy mass and metallicity demonstrated in Tremonti et al. (2004) and the LSN preference for low-mass hosts could imply that metallicity has an influence on the stellar initial mass function (IMF). The preference for low-mass hosts exhibited by these extreme SNe could also be a natural consequence of an increase in the efficiency of metal-line-driven stellar winds that lower the final masses of these same objects in larger galaxies and consequently produce lower-luminosity explosions (see, e.g., Arcavi et al. 2010). The extreme masses of the LSN progenitors in low-mass galaxies offer the opportunity to test models of the IMF that posit distributions limiting the most massive star based on available star-forming gas (Pflamm-Altenburg et al. 2007; Weidner et al. 2010).

Three scenarios have been explored that can produce LSNe: the large production of radioactive fuel produced from the thermonuclear burning of a massive oxygen core that is instigated by a pulsational electron–positron pair instability (PISNe; Barkat et al. 1967; Bond et al. 1984; Heger & Woosley 2002; Waldman

2008), the interaction of the outburst with a dense circumstellar envelope either left over from progenitor formation (Metzger 2010) or produced by late-time mass-loss from the progenitor (Gal-Yam et al. 2007; Smith et al. 2007, 2008), and the energy from a rapidly rotating magentar formed in the collapse of the LSN progenitor star (Kasen & Bildsten 2010; Woosley 2010). The first two scenarios naturally imply extreme masses for the progenitors of LSNe, in some cases in excess of 150 $M_{\odot}$ (Gal-Yam et al. 2009).

Theoretical treatments of the magnetar scenario predict the basic form of observed LSN light curves (Kasen & Bildsten 2010; Woosley 2010), but have yet to provide predictions of detailed spectral features, unlike the pair-production theory which matches the light curves (Scannapieco et al. 2005) and predicts the production of Fe-group elements that have been observed (Gal-Yam et al. 2009). Without these predictions it is yet unclear how many, if any, of the LSNe are magnetar-powered. The same wind-driven mass loss (WDML) and hence correlation with host metallicity and mass could operate in this scenario, if it turns out that magnetar progenitors are also highly massive. The mass of magnetar progenitors is currently being debated in the literature (Klose et al. 2004; Gaensler et al. 2005; Muno et al. 2006; Davies et al. 2009) and range from $\sim$20 to $\geqslant$50 $M_{\odot}$. Until we can confirm that magnetars have actually powered an LSN, it is safer to make the assumption that the LSNe arise from very massive progenitors.

From a galaxy evolution standpoint, the formation of massive stars in low-mass dwarf galaxies implies the very high density star formation typically found in UV-luminous galaxies (UVLGs; Hoopes et al. 2007) and local Lyman-break analogs (LBAs; Overzier et al. 2009). The LSN hosts may delimit the low-luminosity, low-mass, low-metallicity range of these extreme compact starbursting objects that have not yet made it into current UVLG and LBA samples. It is thus important to compare the properties of the LSN hosts with those of the UVLGs and LBAs.

We begin the examination of LSN local environments by comparing the hosts of 17 of the most luminous SNe on record with a sample of 26,000 galaxies from a cross-match (Wyder et al. 2007) between the Sloan Digital Sky Survey (SDSS) spectroscopy catalog and the *Galaxy Evolution Explorer* (*GALEX*; Martin et al. 2005) IR1.1 catalogs. We use UV and optical photometry of the hosts to fit star formation history (SFH) models and estimate their luminosity-weighted age ($\langle \mathrm{Age} \rangle_{\mathrm{L}}$), stellar mass ($M_*$), and current star formation rate (SFR). We compare the distributions of the LSN hosts with the larger sample on the galaxy NUV $- r$ versus M_r color–magnitude diagram (CMD) and a diagram plotting specific star formation rate (sSFR $=$ SFR/M$_*$) versus M_* to demonstrate their extreme nature and to explore other relationships between the LSN subtypes and their host properties. We also compare the SFR of the LSN hosts with models that relate SFR to the IMF (Pflamm-Altenburg et al. 2007) to estimate the probability of producing the high-mass stars capable of producing LSNe.

2. DATA

Our initial sample of 17 LSNe consists of all those discovered to date with $M_V < -21$ as derived from modern (post-1990) photometry (Richardson et al. 2002; Quimby et al. 2007, 2010; Ofek et al. 2007; Smith et al. 2008; Yuan et al. 2008; Miller et al. 2009; Gezari et al. 2009; Gal-Yam et al. 2009; Drake et al. 2010; Pastorello et al. 2010). Our sample includes the LSNe produced by the interaction of the explosion ejecta and the surrounding circumstellar matter. This subgroup is characterized by narrow emission lines in their spectra and are called Type IIn-lum. Two of our sample (SN1999as and SN2007bi) have been determined to be PISNe by their light curves and by showing Fe-group elements in their spectra (Gal-Yam et al. 2009) and are labeled Ic-PP. The other class of LSN studied here we label Type Ipec, which denotes the lack of H emission in their spectra and their peculiar properties (spectra and light curve) when compared with any other SN type (Quimby et al. 2009). These are possibly pulsational PISNe as well (Quimby et al. 2009), but their spectra and light curves do not allow a conclusive classification.

For a comparison sample we use the cross-match between the spectral sample of SDSS DR4 and the *GALEX* G1 interim release IR1.1 catalog presented in Wyder et al. (2007). The basic sample criteria limit the apparent SDSS r-band magnitude of this sample to 17.6 and limit the redshift to $0.01 < z < 0.25$. The NUV completeness for blue galaxies on the faint end is $\sim$90% for this sample, while the NUV faint limit does lead to higher incompleteness for faint red galaxies. For more details on the sample selection, see Section 2.2 of Wyder et al. (2007).

The apparent magnitudes of the LSN hosts are much fainter than this larger sample. In addition, seven of the seventeen LSN hosts are outside the sample redshift range. Our goal in this initial study is not to measure the relative frequency of LSN hosts in the local universe. Our goal is, instead, to place the LSN hosts in a galaxy evolution context as mapped out on the galaxy CMD using a well-measured local sample. We also aim to illustrate that the LSNe are useful for selecting active dwarf galaxies that would ordinarily go undiscovered.

To characterize the hosts of the LSNe, we take advantage of the close correlation between UV luminosity and SFR (Treyer et al. 2007; Salim et al. 2007; Martin et al. 2007). We use archival *GALEX* (Martin et al. 2005) FUV ($\lambda_c = 1539$ Å, $\Delta\lambda = 442$ Å), and NUV ($\lambda_c = 2316$ Å, $\Delta\lambda = 1060$ Å) images and co-add them together to obtain the deepest image possible of the LSN hosts. We add optical photometry to the spectral energy distribution (SED) characterization where available. Our primary source for optical imaging of the hosts is the SDSS (York et al. 2000) Data Release 7.[15] We do not use SDSS catalog photometry, but instead measure the images ourselves, allowing us to match the apertures in each waveband. We supplement our SDSS image photometry with measurements presented in Germany et al. (2000) for SN1997cy, deep photometry of the Coma Cluster by Adami et al. (2006) for SN2005ap, and images from the DeepSky Survey[16] (Nugent et al. 2009) for SN1995av and SN2008fz. Matched apertures are used to characterize the host SED and to derive magnitudes or detection limits in each waveband. A selection of images focusing on the detected hosts is presented in Figure 1.

Table 1 presents the basic data for the LSNe: IAU designation, type, redshift, and host name, followed by the NUV exposure time and observed NUV and r-band magnitudes of the host galaxies. The host names beginning with "A" denote an anonymous galaxy with the rest of the name specifying the J2000 position. In the cases where the host is not detected, the position is of the LSN. A K-correction is made (see Section 2.1) and the K-corrected NUV and r-band values form the final two columns of the table. All the LSNe but SN2006gy appear in anonymous or SDSS galaxies (see Section 4.2). We have detections in the

[15] http://www.sdss.org/dr7/
[16] http://supernova.lbl.gov/~nugent/deepsky.html

Table 1
Luminous SN Host Photometry

SN	Type	z	HOST	Exptime	Observed		K-corrected ($z = 0.1$)	
				NUV (s)	NUV Mag	r Mag[a]	NUV Mag	r Mag[a]
1995av	IIn-lum[b]	0.300	A020136.0+033855.0	440	>22.92	>22.80[c]	>22.62	>22.45[c]
1997cy	IIn-lum	0.063	A043255.1 − 614300.0	1811	19.95 ± 0.04	19.72 ± 0.20[d]	19.95 ± 0.04	19.72 ± 0.20[d]
1999as	Ic-PP	0.127	SDSS J091630.79+133906.1	358	20.42 ± 0.13	19.20 ± 0.08	20.42 ± 0.13	19.20 ± 0.08
1999bd	IIn-lum	0.151	SDSS J093029.10+162607.1	247	21.88 ± 0.27	19.81 ± 0.14	21.88 ± 0.27	19.81 ± 0.14
2000ei	IIn-lum[b]	0.600	SDSS J041707.06+054551.8	2147	>21.73	22.75 ± 0.71	>20.93	21.60 ± 0.71
2005ap	Ipec	0.283	A130113.1+274334.4	4123	>23.49	23.71 ± 0.25[e]	>23.19	23.36 ± 0.25[e]
2006gy	IIn-lum	0.019	NGC1260	21783	17.89 ± 0.02	12.08 ± 0.01	17.89 ± 0.02	12.08 ± 0.01
2006tf	IIn-lum	0.074	SDSS J124615.80+112555.5	3298	21.43 ± 0.07	20.75 ± 0.34	21.43 ± 0.07	20.75 ± 0.34
2007bi	Ic-PP	0.128	SDSS J131920.14+085543.7	202	21.37 ± 0.27	22.41 ± 0.76	21.37 ± 0.27	22.41 ± 0.76
2008am	IIn-lum	0.234	SDSS J122836.31+153449.5	2167	21.02 ± 0.06	19.93 ± 0.14	20.82 ± 0.06	19.73 ± 0.14
2008es	IIn-lum	0.202	A115649.0+542725.0	0	...	>21.71	...	...
2008fz	IIn-lum	0.133	A231616.5+114248.5	192	21.01 ± 0.23	>21.33[c]	21.01 ± 0.23	>21.33[c]
SCP06F6	Ipec	1.189	A143227.4+333224.8	69291	>25.98	>22.80	>24.88	>20.80
PTF09atu	Ipec	0.501	A163024.5+233825.0	543	>22.93	>22.61	>22.23	>21.61
PTF09cnd	Ipec	0.258	A161209.0+512914.5	1951	23.19 ± 0.22	>21.67	22.89 ± 0.22	>21.37
2009jh	Ipec	0.349	A144910.1+292511.4	3249	>24.34	>21.77	>23.94	>21.37
2010gx	Ipec	0.230	SDSS J112546.72 − 084942.0	423	>23.09	22.42 ± 0.24	>22.89	22.22 ± 0.24

Notes.
[a] SDSS r band, unless otherwise noted.
[b] Classification uncertain.
[c] Derived from DeepSky photometry (Nugent et al. 2009).
[d] Derived from photometry presented in Germany et al. (2000).
[e] Derived from photometry presented in Adami et al. (2006).

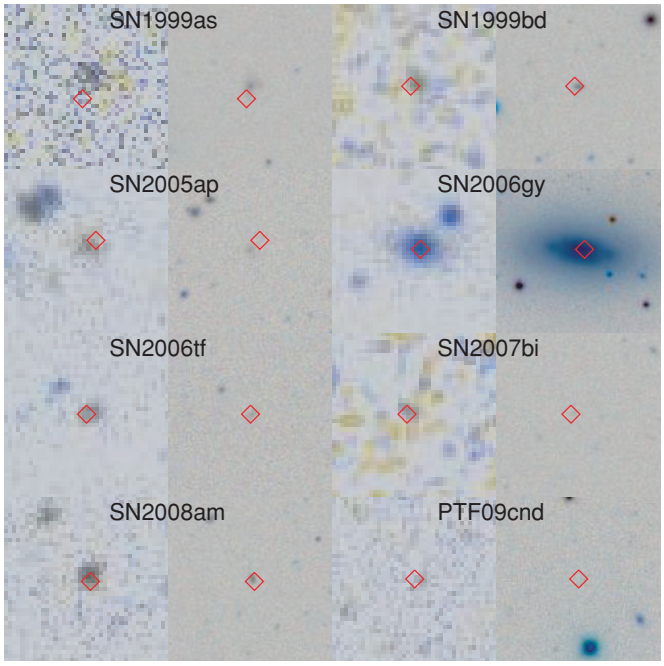

Figure 1. *GALEX* FUV/NUV psuedo-three color images (left panels) and SDSS images (right panels) of the detected hosts of the extreme supernovae. Each panel is one arcminute across. The red diamond marks the location of the supernova. The real host of SN2005ap is blended with a nearby galaxy (see Quimby et al. 2007), so the *GALEX* images were used to determine an upper limit.
(A color version of this figure is available in the online journal.)

NUV for nine of the seventeen hosts and upper limits for all but one of the remaining hosts. SN2008es is near an UV-bright star preventing *GALEX* observations, therefore no NUV upper limit could be derived. For the SDSS r band, we have detections for eight of the seventeen hosts and upper limits for five. The host of SN1997cy was measured by Germany et al. (2000) with V- and R-band imaging. The host of SN2005ap was detected in the broadband (B- and V-band) catalog presented in Adami et al. (2006) which we converted to an approximate r-band magnitude. We use the DeepSky imaging to place upper limits on the r-band luminosity of the hosts of SN1995av and SN2008fz. We had to make assumptions about the SEDs for hosts that were not in the SDSS survey to convert them to an approximate r band. We increase their photometric uncertainties to reflect this situation. All magnitudes have been corrected for foreground extinction (Schlegel et al. 1998) using the reddening law of Cardelli et al. (1989).

2.1. K-correction

To account for the range in redshift of the LSN hosts and facilitate comparison with the Wyder sample, we K-correct each of our SN hosts to the reference redshift of $z = 0.1$ used in Wyder et al. (2007). Since many of our SN hosts are difficult to measure, we use the seven-band UV-optical photometry and redshifts available for the Wyder sample galaxies. We derive K-corrections for the SN hosts by producing a separate galaxy CMD for each SN host, with the Wyder galaxies K-corrected to the redshift of the SN host. We then compare the diagram at the host redshift with the diagram at $z = 0.1$ to derive an approximate K-correction. To perform the K-correction on the Wyder galaxies, we use the latest version of the K_CORRECT program (Blanton & Roweis 2007) which incorporates the *GALEX* bandpasses. We estimate that the corrections can be made in this way to an accuracy of 0.25 mag. For hosts with $z < 0.2$, no correction is made. Columns 8 and 9 of Table 1 give the K-corrected magnitudes and errors (not including the K-correction error).

2.2. Ages, Masses, and Star Formation Rates

For the comparison sample, we use the K-corrected, extinction-corrected NUV luminosities to estimate their recent ($\lesssim 10^8$ yr) SFR (Treyer et al. 2007; Salim et al. 2007). These

Table 2
Luminous SN Host Derived Properties

SN	Type	Host	Age−	⟨Age⟩$_L$	Age+	$M*-$	⟨$M*$⟩	$M*+$	SFR−	⟨SFR⟩	SFR+	sSFR−	⟨sSFR⟩	sSFR+
				(log yr)			(log $M_\odot$)			(log $M_\odot$ yr^{-1})			(log yr^{-1})	
1995av	IIn-lum	A020136.0+033855.0	6.78	8.07	9.99	6.75	8.11	9.69	< −3.00	−0.21	0.22	< −12.00	−8.32	−6.53
1997cy	IIn-lum	A043255.1 − 614300.0	7.45	7.82	8.15	7.96	8.13	8.27	−0.56	−0.34	−0.18	−8.83	−8.47	−8.14
1999as	Ic-PP	SDSS J091630.79+133906.1	7.18	7.28	7.88	8.85	8.95	9.16	0.49	0.59	0.81	−8.68	−8.36	−8.04
1999bd	IIn-lum	SDSS J093029.10+162607.1	7.58	7.88	9.31	9.09	9.33	9.86	−0.38	0.92	1.06	−10.24	−8.42	−8.03
2000ei	IIn-lum	SDSS J041707.06+054551.8	6.78	6.78	9.88	8.73	9.17	11.16	< −3.00	0.79	2.07	< −12.00	−8.39	−6.65
2005ap	Ipec	A130113.1+274334.4	6.78	9.55	9.99	7.60	9.73	9.90	< −3.00	−0.52	0.48	< −12.00	−10.25	−7.13
2006gy	IIn-lum	NGC1260	9.68	9.97	10.10	11.22	11.35	11.44	< −3.00	< −3.00	< −3.00	< −12.00	< −12.00	< −12.00
2006tf	IIn-lum	SDSS J124615.80+112555.5	6.90	7.43	8.15	7.87	8.21	8.55	−0.51	−0.14	0.16	−9.06	−8.35	−7.71
2007bi	Ic-PP	SDSS J131920.14+085543.7	6.78	7.11	8.95	6.56	7.07	8.03	−1.97	−1.29	−0.48	−10.01	−8.37	−7.04
2008am	IIn-lum	SDSS J122836.31+153449.5	6.95	7.54	8.32	9.12	9.41	9.64	0.60	1.07	1.20	−9.04	−8.34	−7.92
2008es	IIn-lum	A115649.0+542725.0	7.98	8.15	8.32	1.00	5.74	8.23	< −3.00	−2.58	−0.20	< −12.00	−8.32	> −6.00
2008fz	IIn-lum	A231616.5+114248.5	6.78	6.90	10.06	1.00	6.71	9.01	< −3.00	−1.67	−0.43	< −12.00	−8.38	> −6.00
SCP06F6	Ipec	A143227.4+333224.8	6.78	8.27	9.67	1.00	9.31	12.03	< −3.00	0.74	1.20	< −12.00	−8.57	> −6.00
PTF09atu	Ipec	A163024.5+233825.0	6.78	6.78	9.73	1.00	7.30	10.07	< −3.00	−1.09	0.50	< −12.00	−8.39	> −6.00
PTF09cnd	Ipec	A161209.0+512914.5	6.78	7.88	9.11	7.57	8.15	9.05	−0.80	−0.18	0.23	−9.85	−8.33	−7.34
2009jh	Ipec	A144910.1+292511.4	6.78	7.75	9.97	1.00	7.40	9.76	< −3.00	−0.94	−0.14	< −12.00	−8.34	> −6.00
2010gx	Ipec	SDSSJ112546.72 − 084942.0	6.78	8.19	9.18	7.67	8.38	8.95	−1.15	−0.38	0.11	−10.10	−8.76	−7.56

methods assume the universal IMF specified in Section 2.2 of Kroupa (2001) with a mass range of 0.1–100 $M_\odot$. The internal extinction is estimated using the Balmer decrement and stellar masses are estimated using spectral fitting. For the details of these calculations see Wyder et al. (2007).

Since we do not have spectra of the LSN host galaxies, we cannot use the same method to derive masses and SFRs. Instead, we use SED fitting to models of SFH. To do this we use the known redshifts and all available photometry and detection limits of the LSN hosts to fit a particular SFH, from which we estimate host ⟨Age⟩$_L$, M_*, and SFR. This is accomplished with the ZPEG program, which uses the PEGASE.2 galaxy evolution code (Fioc & Rocca-Volmerange 1997; Borgne & Rocca-Volmerange 2002; Borgne et al. 2004). The SFR is also derived using the universal IMF from Kroupa (2001). The models assume exponentially declining SFHs with over 100 time steps. Only models that are consistent with the redshift of the host (i.e., younger than the universe at that redshift) are considered in the fitting of the SED. The metallicity of a given model is evolved self-consistently (Fioc & Rocca-Volmerange 1997). A variety of dust prescriptions were used producing over 100 different SEDs that were evolved resulting in a grid of over 10^4 models. For details on the dust prescriptions and SFH models, see Sullivan et al. (2006, Section 3.2) and Sullivan et al. (2010, Section 2.4). The results of the fitting are presented in Table 2 where we repeat the IAU designation, type and host name for each LSNe, followed by the ranges and most probable values of ⟨Age⟩$_L$, M_*, SFR, and sSFR for each host.

To estimate any systematic difference between these two methods, we use the NUV luminosities and NUV − r colors to estimate internal extinction (Treyer et al. 2007) and derive an SFR for each LSN host. We find an error-weighted offset between the two SFR methods for the LSN hosts of ΔSFR[log(M$_\odot$ yr^{-1})](SED − UV) = 0.54 ± 0.10. While this is smaller than the scatter in the SFRs from Table 2, we might be tempted to apply this offset to align the LSN hosts with the comparison sample, even though we have no way to do the same for stellar masses. Unfortunately, the situation for extreme galaxies is complicated and estimating SFR for extremely blue (NUV−r < 1) galaxies shows a high scatter (see Figure 10 in Treyer et al. 2007). For this reason, we do not apply any correction. In addition, with the large photometric errors of these faint hosts, it is difficult to assess which method is more reliable.

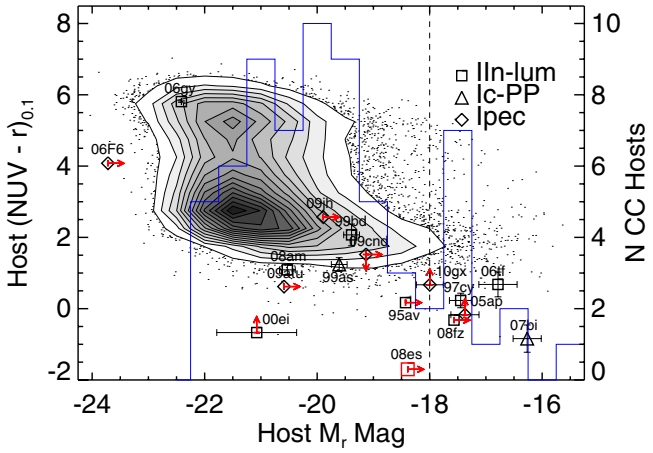

Figure 2. Galaxy CMD with hosts of extreme SNe indicated. The contours represent the density of galaxies from the *GALEX*–SDSS cross-match in Wyder et al. (2007) using photometry that is corrected for Milky Way extinction, K-corrected to a redshift of $z = 0.1$ (see the text), but uncorrected for internal extinction. The arrows indicate limiting magnitudes derived from existing image data. The arrows pointing right limit the host position to a half-plane to the right of the plotted point. The arrows pointing up limit the color to redward of the plotted point. The double arrows for the host of PTF09cnd limit it to a quarter-plane fainter in M_r and blueward of the plotted point. The blue histogram plots the CC SN host M_r distribution from Arcavi et al. (2010) referring to the right axis. The vertical dashed line is the demarcation between "giant" and "dwarf" host galaxies used in that study.

(A color version of this figure is available in the online journal.)

3. RESULTS

We plot the 17 LSN hosts on the galaxy NUV − r versus M_r CMD in Figure 2. The contours represent the galaxy density of the ∼26,000 galaxies from Wyder et al. (2007) in the diagram in 0.5 × 0.5 mag bins in color and luminosity with the darkest level at a density of 1056 galaxies per bin and the lightest level at 132 galaxies per bin. Below the lowest contour density, the galaxies are plotted individually as small dots. We code the symbol for

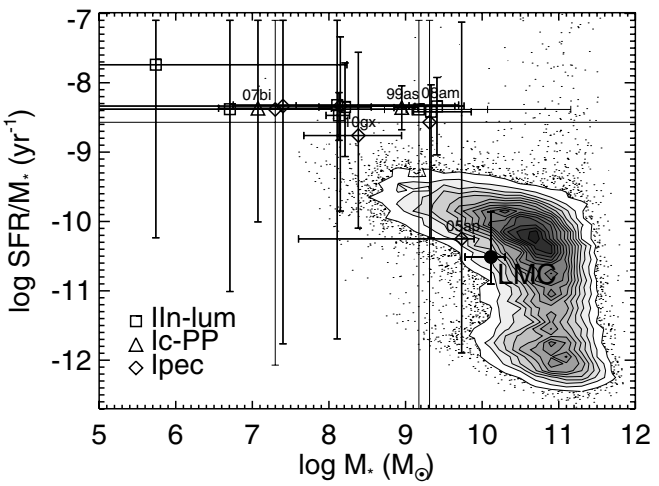

Figure 3. Specific star formation rate as a function of stellar mass for the LSN hosts with a selection of the LSNe labeled to avoid confusion due to overlap. The better constrained hosts have thicker error bars. The contours represent the density of the larger sample of galaxies from the *GALEX*–SDSS cross-match in Wyder et al. (2007; see Figure 2). The LMC is plotted for reference using values from Westerlund (1997) and Harris & Zaritsky (2009).

each SN by type: square for IIn-lum, diamond for Ipec, and triangle for Ic-PP. For comparison, we plot the distribution of M_r host magnitudes for the CC SN sample from Arcavi et al. (2010) which refers to the right axis of the figure. Since this distribution is derived from an areal survey, it should reflect an unbiased sampling of the parent distribution of CC SN host magnitudes.

For SN hosts for which we only have an upper limit, we use (red) arrows to indicate what the allowable range of magnitudes or colors is restricted to. These arrows indicate that with upper limits in both NUV and r, we can only restrict a half-plane in this diagram. For these limits, the symbol is plotted at the position calculated from the color and luminosity of the limiting magnitudes. Four of the limiting cases are unusual. For PTF09cnd, we have a detection in the NUV, but no detection in the r (see Figure 1). This allows us to limit the color and luminosity to a quarter-plane blueward of and fainter in M_r than the plotted symbol. For SN2008es, we have no NUV data (see Section 2), but our r-band limit still restricts the allowable M_r. Therefore, we place the type symbol (red) and identification along the bottom edge of the diagram. For SN2005ap and SN2010gx, the optical detections allow us to measure M_r, but the limits in NUV only allow us to limit the NUV $-$ r color to be redward of (above) the symbol.

We now examine the physical conditions within the host galaxies and plot the 17 LSN hosts on a diagram of sSFR versus M_* in Figure 3. The contours for the larger sample in this case are derived in two-dimensional bins of 0.2 dex wide in M_* and 0.1 dex wide in sSFR. The darkest contour represents a density of 282 galaxies per bin and the lightest contour 17 galaxies per bin, with individual galaxies plotted below this density. The symbol coding for the LSN hosts is the same as in Figure 2. For comparison, we plot the Large Magellanic Cloud (LMC) as the solid circle, using the mass range reported in Westerlund (1997) and the current SFR from Harris & Zaritsky (2009). Since we are comparing individual galaxies to the larger sample, we do not apply a volume correction to the larger sample. This accounts for the difference between our Figure 3 and Figure 26 from Wyder et al. (2007).

4. DISCUSSION

Figures 2 and 3 together support the notion that there is an environmental factor in the production of LSNe. Their distribution in the figures tends toward extreme regions of low luminosity, blue NUV $-$ r, low mass, but high sSFR in spite of having low SFR. Undoubtedly there is incompleteness in the larger sample, but it is hard to imagine a scenario where incompleteness dominates the distribution of the LSNe, given that many fainter SNe are found in more luminous galaxies (Arcavi et al. 2010), and that these more luminous galaxies were preferentially surveyed for decades before areal SN searches were feasible. The incompleteness in the larger sample limits our ability to say just how rare the LSN hosts are, but with upcoming deeper, wide-field, multi-band surveys, the incompleteness limits will be pushed fainter and allow us to measure their volumetric density. For now, the presence of an LSN within a low-luminosity host indicates that the host is undergoing an episode of active, high-density, high-mass star formation. The extreme luminosity of LSNe, allowing them to be detected to high redshift, makes LSN guides for our exploration of star formation in dwarf galaxies over a range of redshifts.

4.1. The Galaxy CMD

Looking at Figure 2 in detail shows that our sample is not large enough to distinguish the LSN host M_r distribution from the full CC host M_r distribution shown in Arcavi et al. (2010). If we divide the sample at the central minimum in the Arcavi distribution ($M_r = -19$) and exclude SN2006gy (see Section 4.2) and SCP06F6 (because of its high redshift and very uncertain K-correction), we count seven hosts brighter than this value and eight hosts fainter. Three of the brighter hosts are upper limits and some or all could be counted in the fainter group. Clearly nothing conclusive can be derived from this, but it begs for deeper photometry and larger samples to see if the LSN hosts are drawn from a different, lower luminosity parent population than the other CC SN hosts.

We also do not see a definitive separation between IIn-lum hosts and Ipec or Ic-PP hosts. The SNe IIn-lum must have had some level of mass loss in order to produce the narrow lines in their spectra from circumstellar interaction. This could have resulted from WDML or from binary interaction or a combination of the two. If IIn-lum hosts are systematically more massive and hence more metal rich (Tremonti et al. 2004) than the type I LSNe, this would imply that WDML is the dominant source of the circumstellar matter and that the metals in the outer atmosphere have their source in the host galaxy itself. If, however, there is an intrinsic source of metals in the stellar evolution of the progenitor from atmospheric dredge-up or the material was ejected due to binary interaction, then the SNe IIn-lum could be found in hosts of any mass. Four of the brightest type I SN hosts in Figure 2 have only limits on M_r and could move to fainter hosts leaving some of the IIn-lums by themselves in brighter hosts. Once again, only deeper photometry and a larger sample will bring this relationship into focus.

4.2. The sSFR Versus M_* Diagram

Figure 3 illustrates the extreme nature of the LSN hosts. The error bars are large because in many cases our estimation of the host SFH is derived from detection limits. The grouping of the hosts near sSFR ~ -8.4 is caused by the combination of a finite time step in the SFH models and the shortest lifetime of stars with SEDs that peak in the UV ($\sim 10^8$ yr). With smaller

time steps and age indicators more sensitive to shorter timescales (e.g., Hα), the most likely values for sSFR might be even higher. Nearly every host is less massive and has a higher sSFR than the LMC. The exception is SN2006gy (see Table 2), which appears in NGC1260, a peculiar S0/Sa galaxy. It has been pointed out that the site of SN2006gy is dusty (Ofek et al. 2007; Miller et al. 2010) and that the infrared luminosity of the host implies an SFR that is not inconsistent with the production of high-mass stars (Smith et al. 2007). It is plausible that NGC1260 has recently accreted a star-forming dwarf that is similar to the other LSN hosts.

Given the low mass of the LSN hosts and their short sSFR timescales, it appears that LSNe are produced in the infancy of a galaxy's evolution. The fact that SN2006gy is the only LSN host that appears in a high-mass host also implies that LSNe are typically produced early in a galaxy's life, before encounters with larger galaxies. Young et al. (2010) point out that SN2007bi presents a problem for PISN models that require either H-rich, moderate metallicity progenitors ($Z \simeq Z_{\odot}/3$) or Population III objects with $Z \lesssim Z_{\odot}/1000$ (Langer et al. 2007), because the SN shows no evidence of being H-rich and yet the metallicity of the host is not consistent with producing a Population III progenitor ($12 + \log([\mathrm{O/H}])_{\mathrm{HOST}} = 8.15 \pm 0.13$, Young et al. 2010). It is possible that the chemical evolution in such small dwarf galaxies is heterogeneous and SN2007bi could have formed from a pocket of primordial (Population III) gas. Young et al. (2010) call for better metallicity measurements of the host of SN2007bi, as their measurements were taken while the SN continuum was still present. It may also be important to acquire resolved metallicity measurements to sort out the spatial pattern of chemical enrichment in these young dwarf galaxies.

If we compare the LSN hosts with the supercompact UVLGs from Hoopes et al. (2007), we see that they share the same range of sSFR and have similar UV-optical colors. The most massive LSN hosts are consistent with the mass range for the supercompact UVLGs, but a large fraction of the LSN hosts are less massive. It is interesting to note that many of the LSN hosts have masses similar to individual star-forming clumps in a sample of LBAs measured in Overzier et al. (2009). This implies that LSN hosts may delineate the low-mass tail of the LBAs, or that they are building blocks from which LBAs and UVLGs are constructed through mergers.

4.3. LSNe and the Stellar IMF

Finding stars as massive as any formed in the Milky Way in galaxies that are many orders of magnitude smaller has strong implications for our understanding of the upper end of the IMF. It is exceedingly difficult to measure individual stellar masses in any but the nearest galaxies, so the LSNe offer the opportunity to test and calibrate theories of the IMF.

To illustrate the potential impact of LSNe on our understanding of the IMF, we examine a recent theory based on the notion that the IMF in a given galaxy is the result of integrating all the IMFs within individual clusters in the galaxy, each of which has an IMF limited by the ongoing star formation (Kroupa & Weidner 2003). This integrated galaxy initial mass function (IGIMF) theory has successfully reproduced many observed properties of high-mass star formation (Pflamm-Altenburg et al. 2007, 2009; Pflamm-Altenburg & Kroupa 2009; Weidner et al. 2010). One standard IGIMF scenario predicts a relationship between the IGIMF and the ongoing SFR which is graphically presented in Figure 4 of Pflamm-Altenburg et al. (2007). This figure presents IGIMF curves for a range of SFRs ranging from 10^{-5} to $10^{2}\ M_{\odot}\ \mathrm{yr}^{-1}$. If we compare the SFRs of the LSN hosts in Table 2 with these curves, we see potential discrepancies for some LSNe depending on what the initial masses are.

We have an estimate for the initial mass of the progenitor of SN2007bi of $>150\ M_{\odot}$, and evidence that it was a single star, i.e., very little circumstellar material (Gal-Yam et al. 2009). Our estimate of the SFR of the host of SN2007bi ranges from $-1.97 < \log M_{\odot}\ \mathrm{yr}^{-1} < -0.48$ which is marginally consistent with the curves presented in Figure 4 of Pflamm-Altenburg et al. (2007) if the initial mass of SN2007bi is $150\ M_{\odot}$ and not greater. The most probable SFRs for many of the LSN hosts are lower than the host of SN2007bi. Discrepancies with the standard scenario of the IGIMF theory could arise if any of the other LSNe have progenitors with initial masses greater than SN2007bi. We must, however, remember that our SFRs for the LSN hosts are derived using methods that assume a single universal IMF (Kroupa 2001; Sullivan et al. 2006). For such small hosts, a single IMF may be appropriate, but this requires spatially resolved imaging of the hosts to see if the majority of the star formation is occurring in a single, large cluster. A discrepancy may indicate simply that the IGIMF curves need to be extended to higher stellar masses. A problem would exist then only if the production of such a high mass star were exceptionally improbable. This could be tested by integrating the IGIMF to the mass of the LSN progenitor and comparing the calculated total mass of the host to the observed mass. Another refinement of this comparison could be achieved by using SFRs based on indicators sensitive to even shorter timescales, i.e., Hα which is sensitive over timescales of $\sim 10^{7}$ yr. The faintness of these hosts would require a significant investment in observing time to achieve this.

On the other hand, any discrepancy could be evidence in favor of lower mass progenitors, perhaps consistent with the magnetar scenario. This consistency for SN2007bi, narrow though it is, is potentially another success for the IGIMF theory. We can see, however, that definitive tests await more accurate LSN progenitor mass estimates and a detailed characterization of the star formation in the host galaxies.

5. CONCLUSIONS

The apparent preference that LSNe have for extreme host galaxies argues for a local environmental effect in their production. The mass–metallicity relationship (Tremonti et al. 2004) and the effect of metallicity on the efficiency of stellar winds argues that WDML is the physical mechanism that prevents LSNe from being produced in more normal, higher metallicity hosts. The extreme nature of the LSN hosts is attested to by comparing their distribution in Figures 2 and 3 with a much larger sample of nearby galaxies from the SDSS–*GALEX* cross-match presented in Wyder et al. (2007). Their distribution in M_r may be different from the general CC host distribution presented in Arcavi et al. (2010), but a measurement of this difference awaits deeper photometry and a larger sample of LSN hosts. Measuring a difference between the hosts of type IIn and type I LSN hosts also awaits better data. The low SFR of the LSN hosts and the possibly high initial mass estimates of the LSN progenitors places them in a crucial location of theoretical diagrams relating the IMF or the IGIMF to ongoing SFR. Potential discrepancies with current theories may exist, but only if typical host SFRs are less than $10^{-1}\ M_{\odot}\ \mathrm{yr}^{-1}$ and progenitor mass estimates significantly exceed $100\ M_{\odot}$.

We gratefully acknowledge the anonymous referee for a careful reading and useful suggestions that improved the presentation of this work.

Joint research by A.G. and M.S. is supported by the Weizmann-UK program. A.G. is also supported by grants from the Israeli Science Foundation, an EU FP7 Marie Curie IRG Fellowship, and a research grant from the Peter and Patricia Gruber Awards.

GALEX (*Galaxy Evolution Explorer*) is a NASA Small Explorer, launched in 2003 April. We gratefully acknowledge NASA's support for construction, operation, and science analysis for the *GALEX* mission, developed in cooperation with the Centre National d'Etudes Spatiales of France and the Korean Ministry of Science and Technology.

This research has made use of the NASA/IPAC Extragalactic Database (NED) which is operated by the Jet Propulsion Laboratory, California Institute of Technology, under contract with the National Aeronautics and Space Administration.

Funding for the SDSS and SDSS-II has been provided by the Alfred P. Sloan Foundation, the Participating Institutions, the National Science Foundation, the U.S. Department of Energy, the National Aeronautics and Space Administration, the Japanese Monbukagakusho, the Max Planck Society, and the Higher Education Funding Council for England. The SDSS Web site is http://www.sdss.org/

The SDSS is managed by the Astrophysical Research Consortium for the Participating Institutions. The Participating Institutions are the American Museum of Natural History, Astrophysical Institute Potsdam, University of Basel, University of Cambridge, Case Western Reserve University, University of Chicago, Drexel University, Fermilab, the Institute for Advanced Study, the Japan Participation Group, Johns Hopkins University, the Joint Institute for Nuclear Astrophysics, the Kavli Institute for Particle Astrophysics and Cosmology, the Korean Scientist Group, the Chinese Academy of Sciences (LAMOST), Los Alamos National Laboratory, the Max-Planck-Institute for Astronomy (MPIA), the Max-Planck-Institute for Astrophysics (MPA), New Mexico State University, Ohio State University, University of Pittsburgh, University of Portsmouth, Princeton University, the United States Naval Observatory, and the University of Washington.

The National Energy Research Scientific Computing Center, which is supported by the Office of Science of the US Department of Energy under Contract No. DE-AC02-05CH11231, provided staff, computational resources and data storage for this project.

REFERENCES

Adami, C., et al. 2006, A&A, 451, 1159
Arcavi, I., et al. 2010, ApJ, 721, 777
Barbary, K., et al. 2009, ApJ, 690, 1358
Barkat, Z., Rakavy, G., & Sack, N. 1967, Phys. Rev. Lett., 18, 379
Blanton, M. R., & Roweis, S. 2007, AJ, 133, 734
Bond, J. R., Arnett, W. D., & Carr, B. J. 1984, ApJ, 280, 825
Borgne, D. L., & Rocca-Volmerange, B. 2002, A&A, 386, 446
Borgne, D. L., Rocca-Volmerange, B., Prugniel, P., Lançon, A., Fioc, M., & Soubiran, C. 2004, A&A, 425, 881
Cardelli, J. A., Clayton, G. C., & Mathis, J. S. 1989, ApJ, 345, 245
Davies, B., Figer, D. F., Kudritzki, R.-P., Trombley, C., Kouveliotou, C., & Wachter, S. 2009, ApJ, 707, 844
Drake, A. J., et al. 2009, ApJ, 696, 870
Drake, A. J., et al. 2010, ApJ, 718, L127
Fioc, M., & Rocca-Volmerange, B. 1997, A&A, 326, 950
Gaensler, B. M., McClure-Griffiths, N. M., Oey, M. S., Haverkorn, M., Dickey, J. M., & Green, A. J. 2005, ApJ, 620, L95
Gal-Yam, A., et al. 2007, ApJ, 656, 372
Gal-Yam, A., et al. 2009, Nature, 462, 624
Germany, L. M., Reiss, D. J., Sadler, E. M., Schmidt, B. P., & Stubbs, C. W. 2000, ApJ, 533, 320
Gezari, S., et al. 2009, ApJ, 690, 1313
Harris, J., & Zaritsky, D. 2009, AJ, 138, 1243
Heger, A., & Woosley, S. E. 2002, ApJ, 567, 532
Hoopes, C. G., et al. 2007, ApJS, 173, 441
Kasen, D., & Bildsten, L. 2010, ApJ, 717, 245
Klose, S., et al. 2004, ApJ, 609, L13
Kozłowski, S., et al. 2010, ApJ, 722, 1624
Kroupa, P. 2001, MNRAS, 322, 231
Kroupa, P., & Weidner, C. 2003, ApJ, 598, 1076
Langer, N., Norman, C. A., de Koter, A., Vink, J. S., Cantiello, M., & Yoon, S.-C. 2007, A&A, 475, L19
Law, N. M., et al. 2009, PASP, 121, 1395
Martin, D. C., et al. 2005, ApJ, 619, L1
Martin, D. C., et al. 2007, ApJS, 173, 415
Metzger, B. D. 2010, MNRAS, 409, 284
Miller, A. A., Smith, N., Li, W., Bloom, J. S., Chornock, R., Filippenko, A. V., & Prochaska, J. X. 2010, AJ, 139, 2218
Miller, A. A., et al. 2009, ApJ, 690, 1303
Muno, M. P., et al. 2006, ApJ, 636, L41
Nugent, P. E. 2009, BAAS, 41, 419
Ofek, E. O., et al. 2007, ApJ, 659, L13
Overzier, R. A., et al. 2009, ApJ, 706, 203
Pastorello, A., et al. 2010, ApJ, 724, L16
Pflamm-Altenburg, J., & Kroupa, P. 2009, ApJ, 706, 516
Pflamm-Altenburg, J., Weidner, C., & Kroupa, P. 2007, ApJ, 671, 1550
Pflamm-Altenburg, J., Weidner, C., & Kroupa, P. 2009, MNRAS, 395, 394
Quimby, R. M. 2006, Proquest dissertations and PhD theses, Univ. Texas at Austin
Quimby, R. M., Aldering, G., Wheeler, J. C., Höflich, P., Akerlof, C. W., & Rykoff, E. S. 2007, ApJ, 668, L99
Quimby, R. M., Kulkarni, S. R., Ofek, E., Kasliwal, M. M., Levitan, D., Gal-Yam, A., & Cenko, S. B. 2010, ATel., 2492, 1
Quimby, R. M., et al. 2009, arXiv:0910.0059
Rau, A., et al. 2009, PASP, 121, 1334
Richardson, D., Branch, D., Casebeer, D., Millard, J., Thomas, R. C., & Baron, E. 2002, AJ, 123, 745
Salim, S., et al. 2007, ApJS, 173, 267
Scannapieco, E., Madau, P., Woosley, S., Heger, A., & Ferrara, A. 2005, ApJ, 633, 1031
Schlegel, D. J., Finkbeiner, D. P., & Davis, M. 1998, ApJ, 500, 525
Smith, N., Chornock, R., Li, W., Ganeshalingam, M., Silverman, J. M., Foley, R. J., Filippenko, A. V., & Barth, A. J. 2008, ApJ, 686, 467
Smith, N., et al. 2007, ApJ, 666, 1116
Sullivan, M., et al. 2006, ApJ, 648, 868
Sullivan, M., et al. 2010, MNRAS, 406, 782
Tremonti, C. A., et al. 2004, ApJ, 613, 898
Treyer, M., et al. 2007, ApJS, 173, 256
Waldman, R. 2008, ApJ, 685, 1103
Weidner, C., Kroupa, P., & Bonnell, I. A. D. 2010, MNRAS, 401, 275
Westerlund, B. E. 1997, The Magellanic Clouds (Cambridge Astrophys. Series, Vol. 29; Cambridge: Cambridge Univ. Press)
Woosley, S. E. 2010, ApJ, 719, L204
Wyder, T. K., et al. 2007, ApJS, 173, 293
York, D. G., et al. 2000, AJ, 120, 1579
Young, D. R., et al. 2010, A&A, 512, 70
Yuan, F., et al. 2008, CBET, 1262, 1